JOURNAL OF Materials CHEMISTRY

Photoluminescence of new Er^{3+}-doped titanosilicate materials

J. Rocha,*[a] L. D. Carlos,[b] J. P. Rainho,[a,b] Z. Lin,[a] P. Ferreira[a] and R. M. Almeida[c]

[a]*Department of Chemistry, University of Aveiro, 3810 Aveiro, Portugal. E-mail: ROCHA@DQ.UA.PT; Fax: +351 234 370084; Tel: +351 234 370730*
[b]*Department of Physics, University of Aveiro, 3810 Aveiro, Portugal*
[c]*Departamento de Engenharia de Materiais/INESC Instituto Superior Técnico, Av. Rovisco Pais, 1000 Lisboa, Portugal*

Received 20th December 1999, Accepted 27th March 2000
Published on the Web 9th May 2000

Microporous titanosilicate ETS-10 doped with different concentrations of Er^{3+} ions is used as a precursor for preparing novel dense materials, analogues of the mineral narsarsukite, which display a high and stable room temperature emission in the visible and infrared spectral regions. The emission spectra of these phosphors display a visible broad band—associated with the narsarsukite matrix—and a series of narrow intra-$4f^{11}$ $^4I_{13/2}\rightarrow{}^4I_{15/2}$ lines. The number of Stark components detected in Er^{3+}-doped narsarsukite indicates the presence of more than one optically active environment. No significant quenching of luminescence *via* ion–ion or ion–matrix interaction was detected in the range of Er^{3+} concentrations used. The presence of two multiphonon-assisted anti-Stokes excitation sidebands and an energy transfer mechanism between the host lattice and the optically-active Er^{3+} ions demonstrate that the ion–lattice interactions can play an important role in the interesting luminescence properties of these new titanosilicates.

Introduction

In the last decade, the considerable progress achieved in the development of communication systems based on fiberoptics has stimulated a growing interest in light sources emitting at *ca.* 1540 nm.[1–4] This wavelength corresponds to the lowest attenuation and low dispersion of standard silica-based optical fibers, a highly desirable feature for signal transmission through glass fiber cables and for optical on-chip communication.[3,4] Due to its intra-$4f^{11}$ $^4I_{13/2}\rightarrow{}^4I_{15/2}$ transition, trivalent erbium is a good candidate for a temperature-stable emission at 1540 nm.[1–5] ETS-10 is the most prominent member of a recently discovered family of crystalline microporous titanosilicates known as ETS materials,[6,7] presenting considerable potential for applications in shape-selective catalysis,[8] ion-exchange,[9] and as a desiccant material.[10] Here, we wish to report that ETS-10 doped with Er^{3+} ions may be used as a precursor for preparing novel dense analogues of the mineral narsarsukite, which exhibit very interesting luminescence properties. Amorphous luminescent materials have also been synthesized.

ETS-10 [$(Na,K)_2TiSi_5O_{13}\cdot xH_2O$] is a large-pore titanosilicate with a framework consisting of "TiO_2" rods, which run in two orthogonal directions, surrounded by tetrahedral silicate units [Fig. 1(a)].[7] The pore structure consists of 12-rings, 7-rings, 5-rings and 3-rings and has a three-dimensional large-pore channel system whose minimum diameter is defined by 12-ring apertures. The disorder in ETS-10 arises from structural faulting along planes parallel to the 12-ring channel directions, and it is possible to describe the structure in terms of an intergrowth of two ordered polymorphs with tetragonal and monoclinic symmetry. Since ETS-10 contains corner-sharing TiO_6 octahedra and corner-sharing SiO_4 tetrahedra for every framework titanium, there is an associated -2 charge. This charge is compensated for by extra-framework cations, usually Na^+ and K^+.

Upon calcination in air at temperatures in the range 1023–1173 K, ETS-10 transforms into synthetic narsarsukite [$(Na,K)_2TiSi_4O_{11}$], a dense tetragonal titanosilicate mineral[11] made up of Si_4O_{10} chains which form tubes of rings of four SiO_4 tetrahedra. These tubes are linked by chains of corner-sharing TiO_6 octahedra. The cavities between the Si_4O_{10} tubes and octahedral chains contain only Na^+ in the mineral narsarsukite and both Na^+ and K^+ ions in the synthetic material.

In the novel method proposed here for preparing luminescent titanosilicates, the Er^{3+} ions are first introduced into the pores of ETS-10 *via* conventional ion-exchange techniques [Fig. 1(b)]. Then, Er^{3+}-doped ETS-10 is calcined in air at

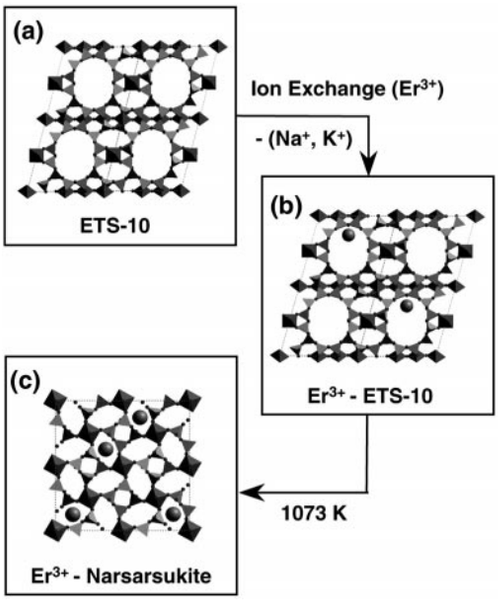

Fig. 1 Preparation of Er^{3+}-doped narsarsukite materials from precursor ETS-10. (a) Parent ETS-10 (Na^+, K^+ and water molecules are omitted for clarity). (b) Er^{3+} cations (solid circle) are introduced into the pores of ETS-10 *via* ion-exchange. The location of these cations is, at present, not known, but it is likely that they reside close to the (negatively charged) TiO_6 octahedra. (c) Upon calcination in air at temperatures in excess of *ca.* 973 K, ETS-10 transforms into synthetic narsarsukite (Na^+ and K^+ are omitted for clarity).

temperatures in excess of *ca.* 973 K, undergoing a phase transformation to synthetic narsarsukite [Fig. 1(c)]. In the process, the Er^{3+} ions are trapped in the narsarsukite lattice. The amount of erbium introduced into this material (and, hence, the distance between two neighboring Er^{3+} ions) can be easily controlled by fine tuning the ion-exchange process.

Experimental

Sample preparation

The synthesis of ETS-10 has been described previously.[6,7,12] The actual sample used in this study contained a small amount of quartz. A typical example of the method used for the introduction of Er^{3+} ions into narsarsukite, yielding a Ti/Er molar ratio of 11 (as ascertained by bulk, ICP, chemical analysis) is as follows: 0.070 g of erbium(III) nitrate pentahydrate (99.9% Sigma-Aldrich) was dissolved in 250 ml distilled water. 3.94 g of as-prepared ETS-10 was then added and the suspension stirred for 24 h at 333 K. The solid was filtered from suspension, thoroughly washed with distilled water and dried at 383 K. The resultant ETS material was re-suspended in a fresh Er^{3+} solution and the entire procedure repeated (second cycle), after which a third ion-exchange cycle was performed. Powder XRD and ^{29}Si MAS NMR analyses show that ETS-10 retains its structural integrity after these treatments. Finally, the Er^{3+}-doped ETS-10 material was placed in a platinum crucible in an oven and calcined in air (heating rate of 5 K min^{-1}) from room temperature to 1073 K, with this final temperature being maintained for 3 h. Two other synthetic narsarsukite samples, with Ti/Er ratios of *ca.* 23 and 9, were prepared by the same method. In a separate study, we attempted to introduce Er^{3+} ions directly into synthetic (undoped) narsarsukite *via* ion exchange. The resultant material did not display any interesting optical properties, presumably because Er^{3+} could not replace the Na^+ and K^+ ions present in as-prepared narsarsukite. Thus, we abandoned this alternative route for preparing luminescent materials.

Techniques

Powder XRD data were collected on an X'Pert Philips MPD system (PW3373/00 Cu LFF X-ray tube) using Cu-Kα ($\lambda = 1.54056$ Å) radiation. A low temperature camera (Paar Physica TTK 450) was used to study the temperature dependence (77–300 K) of the *in situ* powder XRD patterns.

^{29}Si MAS NMR spectra were recorded at 79.49 MHz (9.4 T) on a Bruker MSL 400P spectrometer using 40° pulses, spinning rates of 5.0–5.5 kHz and 120 s recycle delays. Chemical shifts are quoted in ppm from tetramethylsilane (TMS).

Infrared spectra were recorded on a 1 m Czerny-Turner spectrometer (1000 M Spex)—fitted with a 600 grooves mm^{-1} grating blazed at 1600 nm—coupled to a Ge North-Coast EO-817 photodiode cooled to 77 K. The visible spectra were recorded in a 1 m Czerny-Turner spectrometer (1704 Spex)—fitted with a 1200 grooves mm^{-1} grating blazed at 500 nm—coupled to a R928 Hamamatsu photomultiplier. The 325 nm line of an He–Cd laser, an Ar ion-laser (488 and 496.5 nm lines) and a 150 W Xe arc lamp coupled to a 0.25 m excitation monochromator (Kratos GM-252) fitted with a 1180 grooves mm^{-1} grating blazed at 240 nm were used as excitation sources. All the spectra were recorded between 14 and 300 K and were corrected for the response of the detectors.

Results and discussion

Powder XRD and ^{29}Si MAS NMR data show that ETS-10 is stable up to *ca.* 923 K, although at this temperature the samples are poorly crystalline and contain a considerable amount of amorphous siliceous material. Synthetic narsarsukite crystallizes between *ca.* 1023 and 1173 K (Fig. 2 and 3). Because the Si/Ti molar ratio in pure ETS-10 is 5, while in narsarsukite it is 4, the amorphous siliceous materials crystallize as the silica polymorphs, cristobalite and quartz. The ^{29}Si MAS NMR spectrum of narsarsukite (Fig. 3) contains two resonances at −95.2 and −97.8 ppm on a 1 : 1 intensity ratio, assigned to the silicon environment Si(3Si, 1Ti) (that is, silicon connected through oxygen bridges to three tetrahedral silicon atoms and one octahedral titanium atom). However, the structure of ideal tetragonal narsarsukite calls for the presence of a single type of Si and, thus, the structure of the synthetic material must be slightly distorted, thereby lowering the symmetry. This is in accord with results previously reported.[13] Differential thermal analysis (not shown) indicates that the materials melt at *ca.* 1190 K. The powder XRD pattern of a sample calcined at 1223 K and cooled down to room temperature shows the presence of some tridymite (Fig. 2) which (as with quartz) is not clearly detected by ^{29}Si MAS NMR due to a very long spin–lattice relaxation time. The ^{29}Si MAS NMR spectrum of this sample (Fig. 3) displays a broad resonance at *ca.* –96 ppm,

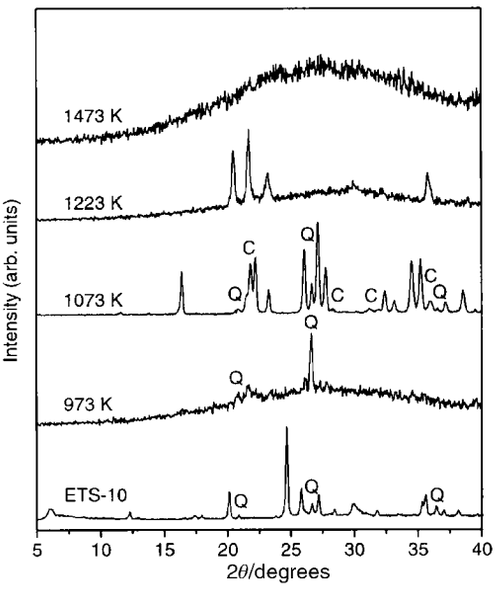

Fig. 2 Powder X-ray diffraction patterns of ETS-10 materials calcined in air at the temperatures indicated. Q and C refer to the quartz and cristobalite impurities, respectively.

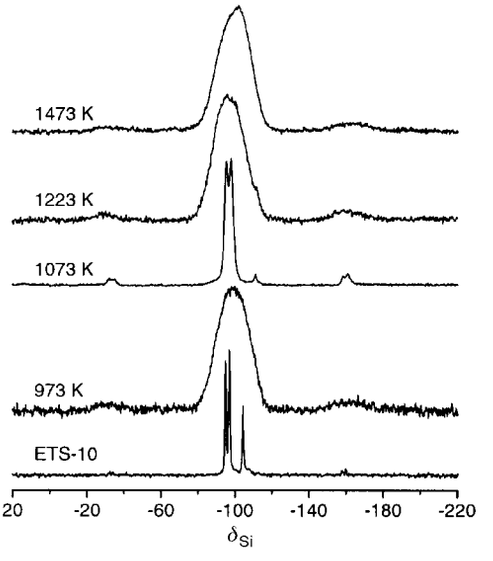

Fig. 3 ^{29}Si MAS NMR spectra of ETS-10 materials calcined in air at the temperatures indicated.

showing that the sample contains a considerable amount of an amorphous siliceous phase. At *ca.* 1473 K, the sample is totally amorphous.

ETS-10 with a Ti/Er ratio of 23 has been calcined at temperatures up to 1473 K. The results are similar to those described above for undoped ETS-10. However, at 973 K, powder XRD (Fig. 4) and ^{29}Si MAS NMR (Fig. 5) data indicate that the Er^{3+}-doped material already contains a significant amount of narsarsukite. This suggests that the presence of Er^{3+} in the pores makes ETS-10 more prone to thermal decomposition. The powder XRD patterns of Er^{3+}-doped ETS-10 calcined at 1073 K (Fig. 4) show that all materials contain narsarsukite contaminated with some quartz and cristobalite, the amounts of which increase with increasing Er^{3+} content. On the other hand, as the Er^{3+} content increases, the ^{29}Si MAS NMR resonances due to these samples (Fig. 6) broaden considerably and the spinning sidebands also become much stronger. This is a clear indication that the narsarsukite materials contain (paramagnetic) Er^{3+} centres in increasing amounts. An Er^{3+}-doped narsarsukite sample (obtained from ETS-10 calcined at 1073 K) was studied by *in situ* powder XRD from 77 to 300 K (not shown). No structural transformations were observed.

Fig. 7 shows an example of the excitation spectra observed for the Er^{3+}-doped ETS-10 materials, Er^{3+}-doped narsarsukite in this case. The sharp lines are assigned to intra-4f^{11} transitions between the $^4I_{15/2}$ and the $^4F_{9/2,7/2,5/2,3/2}$, $^4S_{3/2}$, $^2H_{11/2,9/2}$, $^4G_{11/2}$, $^2K_{15/2}$, and $^2G_{7/2}$ levels. The two bands centred at *ca.* 500 and *ca.* 537 nm are ascribed to multiphonon-assisted anti-Stokes side bands of the $^4F_{7/2}$ and $^2H_{11/2}$ levels, respectively.[14–18] Its integrated intensity increases with increasing temperature, in contrast to the remaining lines (Fig. 7 inset). The energy difference between these lines and the corresponding intra-Er^{3+} electronic levels is provided by the annihilation of simultaneous phonons from the titanosilicate lattice.[14] For trivalent lanthanide ions, the ion–phonon coupling is so weak that, in general, the multiphonon side band absorption cannot be observed by standard absorption spectroscopy and, in most cases, it has been neglected.[14,15] However, after the first report on this process, about 23 years ago,[14] a series of studies have been carried out on crystalline and glassy hosts stressing the important role of anti-Stokes multiphonon sidebands in several optical effects, such as

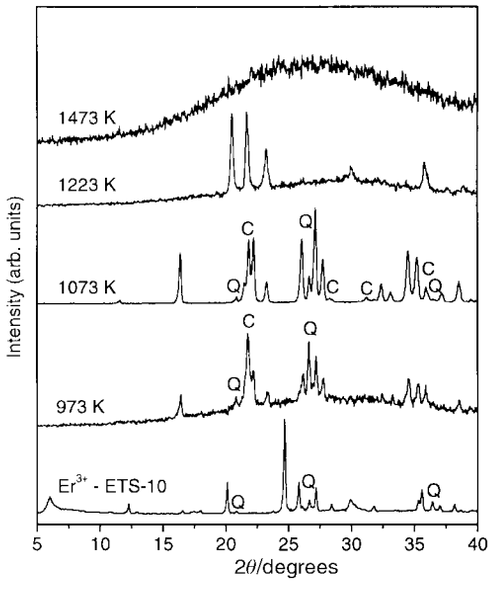

Fig. 4 Powder X-ray diffraction patterns of Er^{3+}-doped ETS-10 materials (Ti/Er = 23) calcined in air at the temperatures indicated. Q and C refer to the quartz and cristobalite impurities, respectively.

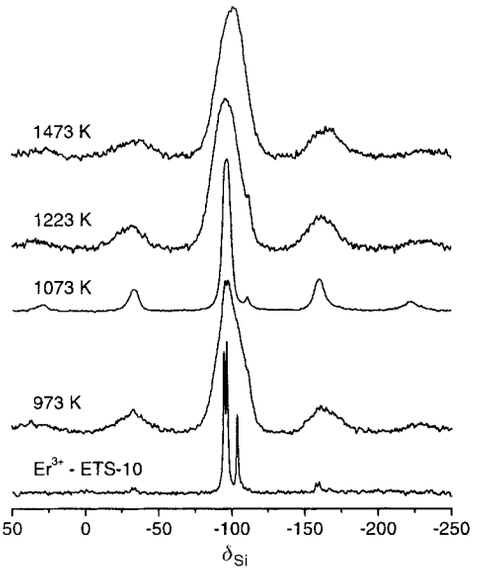

Fig. 5 ^{29}Si MAS NMR spectra of Er^{3+}-doped ETS-10 materials (Ti/Er = 23) calcined in air at the temperatures indicated.

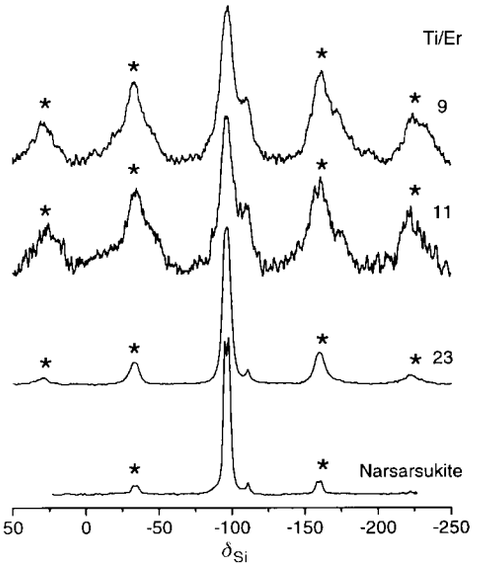

Fig. 6 ^{29}Si MAS NMR spectra of narsarsukite and Er^{3+}-doped narsarsukite, with the Ti/Er molar ratios given. The asterisks denote spinning sidebands. The faint peak at *ca.* –110 ppm is due to a small amount of cristobalite impurity.

avalanche processes,[16] multiphonon-assisted energy transfer,[17] and up-conversion phenomena.[18]

The titanosilicate skeleton of the undoped- and Er^{3+}-doped materials displays luminescence in the visible region of the electromagnetic spectrum. A typical 14 K visible emission spectrum is shown in Fig. 8 for Er^{3+}-doped narsarsukite. The spectrum displays two broad purplish-blue bands centred at *ca.* 414 and *ca.* 443 nm, a green component at *ca.* 520 nm, and two red ones at *ca.* 730 and *ca.* 830 nm. The sharp peaks at 487–489.5, 519–524.5, and 547 nm are due to the Er^{3+} self-absorptions from the host luminescence and are assigned to transitions between the $^4I_{15/2}$ and the $^4F_{7/2}$, $^2H_{11/2}$, and $^4S_{3/2}$ Er^{3+} levels, respectively. At 300 K both the green and red components could not be detected and the spectrum is dominated by the purplish-blue emission. Electron–hole recombinations occurring in the titanosilicate skeleton may be the mechanisms which originate this broad emission.

The room-temperature infrared emission spectra of Er^{3+}-doped ETS-10 materials calcined at 973–1473 K

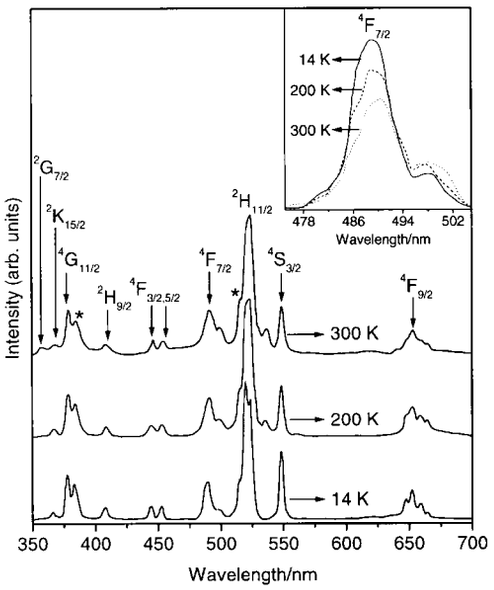

Fig. 7 Excitation spectrum ($\lambda_{emis} = 1542$ nm) of Er^{3+}-doped narsarsukite (Ti/Er = 23) recorded at 14, 200, and 300 K. The asterisks denote possible superposition with the 4th and 3rd emission wavelength submultiples. The inset shows the evolution with temperature for the $^4I_{15/2} \rightarrow {}^4F_{7/2}$ transition and the multiphonon anti-Stokes sideband at *ca.* 500 nm.

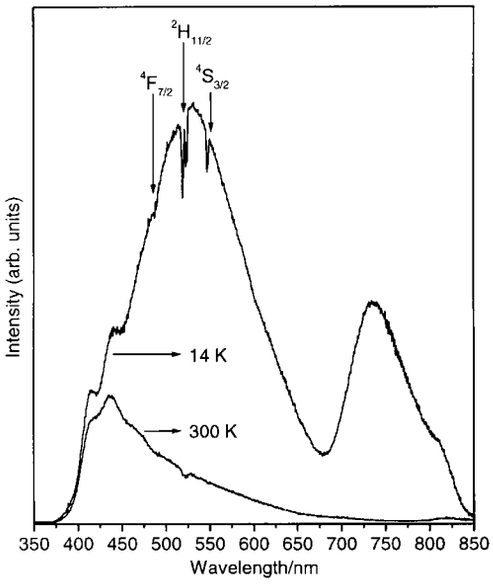

Fig. 8 Visible emission spectra ($\lambda_{exc} = 325$ nm) of Er^{3+}-doped narsarsukite (Ti/Er = 23) recorded at 14 and 300 K.

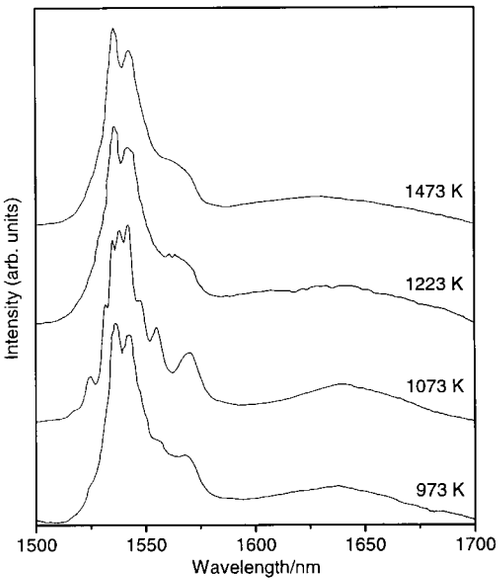

Fig. 9 Infrared room temperature emission spectra ($\lambda_{exc} = 496.5$ nm) of Er^{3+}-doped ETS-10 (Ti/Er = 23) calcined at the temperatures indicated.

($\lambda_{exc} = 496.5$ nm; Fig. 9) display several lines ranging from 1500 to 1650 nm with a main peak at 1543.4 nm. These lines are assigned to the intra-$4f^{11}$ transitions between the $^4I_{13/2}$ and $^4I_{15/2}$ levels of the Er^{3+} ground multiplet. The spectrum of the sample calcined at 1073 K (Er^{3+}-doped narsarsukite) exhibits the best resolved local-field Stark structure (10–11 lines are detected). The full-width-at-half-maximum (FWHM) of the peak at 1543.4 nm for the calcined Er^{3+}-doped ETS-10 materials varies from 14 (1073 K) to a maximum of 23 cm^{-1} (973 K). Similar results were obtained with intra-$4f^{11}$ excitation lines, 488 and 514 nm. Moreover, an efficient room temperature infrared emission is also detected for excitation wavelengths associated with the narsarsukite skeleton emission, *ca.* 325 nm (not shown). This clearly indicates an energy transfer between the narsarsukite host and the optically active Er^{3+} centres. The integrated intensity of the room-temperature Er^{3+}-luminescence does not change appreciably for all the remaining samples calcined between 973 and 1473 K. Er^{3+}-doped ETS-10 and samples calcined at temperatures lower than *ca.* 973 K did not display any detectable infrared luminescence.

When the temperature is decreased from 300 to 14 K (Fig. 10), the Stark structure of the $^4I_{13/2} \rightarrow {}^4I_{15/2}$ transition in Er^{3+}-doped narsarsukite changes and 14 distinct lines are detected. Their FWHM decrease from 8–50 cm^{-1} (300 K) to 4–26 cm^{-1} (14 K). The number of Stark components detected is larger than the expected for Er^{3+} centres in cubic and in lower than cubic symmetry.[1,3,5] This indicates the presence of more than one optically-active Er^{3+} local environment. Moreover, the fact that 7 of the 14 Stark components observed at 14 K are narrower than the remaining lines by a factor of *ca.* 2 suggests that one of the local Er^{3+} environments exhibits a site-to-site variation larger than the other (or others). Despite the presence of impurities (cristobalite and quartz) in Er^{3+}-doped narsarsukite samples, we believe that these phases do not contribute significantly to the observed luminescence features. However, work is in progress to address this problem.

For intra-$4f^{11}$ excitation wavelengths (*e.g.* 488 nm) the temperature dependence of the $^4I_{13/2} \rightarrow {}^4I_{15/2}$ integrated intensity follows a typical Arrhenius-type curve, decreasing with increasing temperature by a factor of *ca.* 1.6 (Fig. 10 inset). We note that this small thermal quenching for the 488 nm excitation wavelength is similar to that reported for Er^{3+}-doped SiO_2 films containing Si nanocrystals[19] and Er^{3+}-doped porous silicon,[20] but much lower (about two or three orders of magnitude) than that observed for Er^{3+}-doped crystalline silicon used in thin-film integrated optoelectronics.[1,2] However, for multiphonon-assisted anti-Stokes excitation (*e.g.* 496.5 nm), the temperature dependence of the $^4I_{13/2} \rightarrow {}^4I_{15/2}$ integrated intensity shows exactly the opposite behavior (Fig. 10 inset). In fact, for excitation energies lower than the $^4F_{7/2}$ excitation the intensity increases by a factor of *ca.* 1.8, when the temperature is raised from 14 to 300 K. This may be certainly related to the increase with temperature of the integrated intensity of the multiphonon-assisted anti-Stokes sideband mentioned in the discussion of the excitation spectrum (Fig. 7). The determination of the local vibrational frequency of this phonon side band and of the magnitude of the electron–phonon coupling parameter is the subject of a forthcoming paper.

Narsarsukite materials containing larger amounts of Er^{3+}

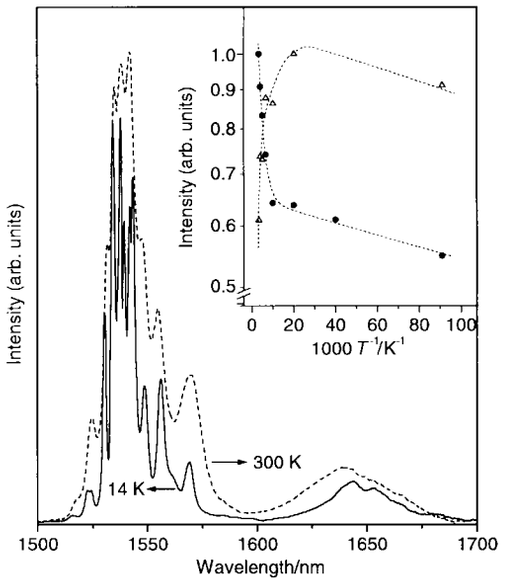

Fig. 10 Infrared emission spectra ($\lambda_{exc}=496.5$ nm) of Er^{3+}-doped narsarsukite (Ti/Er = 23) recorded at 14 (solid line) and 300 K (dashed line). The inset shows an Arrhenius plot of the $^4I_{13/2}\rightarrow{}^4I_{15/2}$ normalized integrated intensity recorded for two excitation wavelengths, 488 (open triangles) and 496.5 nm (solid circles). The lines through the data are guides for the eye.

(Ti/Er = 11 and 9) display similar emission features. In particular, no significant quenching of the $^4I_{13/2}\rightarrow{}^4I_{15/2}$ luminescence *via* ion–ion or ion–matrix interaction was detected in the range of Er^{3+} concentrations studied here (Fig. 11).

Conclusions

In this work, we have reported a new method for preparing luminescent ETS-10 microporous titanosilicates containing Er^{3+}. The metal ions are incorporated into the pores of ETS-10 *via* conventional ion-exchange techniques and the resulting materials calcined in air at a temperature between 823 and 1773 K. The powder XRD and ^{29}Si MAS NMR results show that Er^{3+}-doped ETS-10 samples (calcined and non-calcined) essentially retain the structural integrity of the undoped titanosilicates. As the calcination temperature increases, several phase transformations occur. Upon calcination between 973–1173 K, Er^{3+}-doped narsarsukite crystallizes, at *ca.* 1190 K the materials melt and at *ca.* 1473 K only an amorphous phase is detected by powder XRD and ^{29}Si MAS NMR.

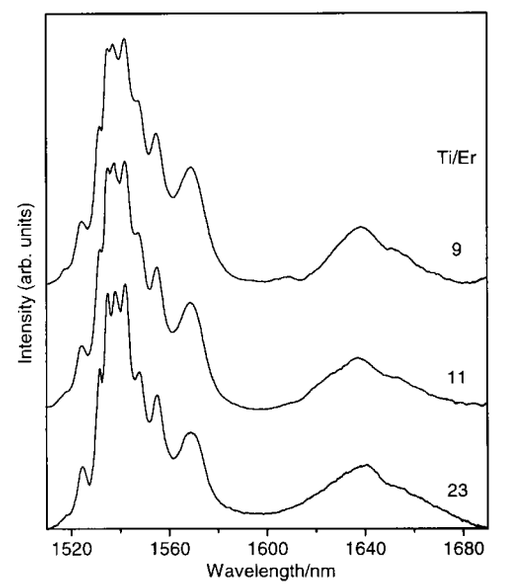

Fig. 11 Infrared room temperature emission spectra ($\lambda_{exc}=496.5$ nm) of Er^{3+}-doped narsarsukite with the Ti/Er molar ratios given.

All the Er^{3+}-doped titanosilicates calcined at temperatures above *ca.* 973 K display a very efficient room temperature 1540 nm luminescence. We should stress that the Er^{3+}-doped glassy sample also shows similar luminescence properties. Moreover, for the range of Er^{3+} concentrations used, no significant differences in the emission features were detected.

In Er^{3+}-doped narsarsukite, an energy transfer mechanism between the narsarsukite skeleton and the optically active Er^{3+}centres seems to occur. This is inferred from: (i) the observed room temperature 1540 nm luminescence when the samples are excited under UV wavelengths associated with the narsarsukite skeleton; (ii) the presence of multiphonon-assisted anti-Stokes excitation sidebands; and (iii) the temperature-dependent deactivation process involved in the conversion of the green and red light emitted by the narsarsukite host into Er^{3+} luminescence (*ca.* 1540 nm). The energy transfer mechanism and the multiphonon-assisted anti-Stokes excitation sidebands point out that, in these materials, the electron–phonon interactions may play a significant role on their luminescence features.

Acknowledgements

The authors wish to thank F. Auzel (CNRS, France) for fruitful discussions and comments concerning the multiphonon-assisted anti-Stokes excitation. Financial support from PRAXIS XXI and FEDER is gratefully acknowledged.

References

1 A. Polman, *J. Appl. Phys.*, 1997, **82**, 1.
2 H. H. Przybylinska, W. Jantsch, Y. Suprun-Belevitch, M. Stepikhova, L. Palmetshofer, G. Hendorfer, A. Kozanecki, R. J. Wilson and B. J. Sealy, *Phys. Rev. B*, 1996, **54**, 2532.
3 X. Orignac, D. Barbier, X. M. Du and R. M. Almeida, *Appl. Phys. Lett.*, 1996, **69**, 895.
4 C. Strohhöfer, J. Fick, H. C. Vasconcelos and R. M. Almeida, *J. Non-Cryst. Solids*, 1998, **226**, 182.
5 G. Dieke, *Spectra and Energy Levels of Rare Earth Ions in Crystals*, John Wiley & Sons, New York, 1965.
6 S. M. Kuznicki, *US Patent* No. 4 853 202, 1989.
7 M. W. Anderson, O. Terasaki, T. Ohsuna, A. Philippou, S. P. MacKay, A. Ferreira, J. Rocha and S. Lidin, *Nature*, 1994, **367**, 347.
8 A. Philippou, J. Rocha and M. W. Anderson, *Catal. Lett.*, 1999, **57**, 151.
9 S. M. Kuznicki and K. A. Thrush, *US Patent* No. 4 994 191, 1991.
10 S. M. Kuznicki, K. A. Thrush and H. M. Garfinkel, *WO Patent* No. 93/00152, 1993.
11 Y. A. Pyatenko and Z. V. Pudovkina, *Kristallografiya*, 1960, **5**, 563.
12 J. Rocha, A. Ferreira, Z. Lin and M. W. Anderson, *Microporous Mesoporous Mater.*, 1998, **23**, 253.
13 M. Naderi and M. W. Anderson, *Zeolites*, 1996, **17**, 437.
14 F. Auzel, *Phys. Rev. B*, 1976, **13**, 2809.
15 F. Auzel and Y. H. Chen, *J. Lumin.*, 1996, **66–67**, 224.
16 F. Auzel and Y. H. Chen, *J. Lumin.*, 1995, **65**, 45.
17 J. P. Jouart and G. Mary, *J. Lumin.*, 1990, **46**, 39.
18 J. P. Jouart, G. Bissieux and G. Mary, *J. Phys. C: Solid State Phys.*, 1987, **20**, 2019.
19 F. Minoru, M. Yoshida, S. Hayashi and K. Yamamoto, *J. Appl. Phys.*, 1998, **84**, 4525.
20 X. Wu, U. Hömmerich, F. Namavar and A. M. Cremins-Costa, *Appl. Phys. Lett.*, 1996, **69**, 1903.